Int J Adv Manuf Technol (2013) 64:1695–1707
DOI 10.1007/s00170-012-4133-0

ORIGINAL ARTICLE

Isoplanar-based adaptive sampling for model-unknown sculptured surface coordinate metrology using non-contact probe

Haibo Liu · Yongqing Wang · Xiaoping Huang · Lin Xue

Received: 25 November 2011 / Accepted: 2 April 2012 / Published online: 26 April 2012

Abstract Optimizing sampling size and point distribution is a difficult issue for sculptured surface measurement. Highly curved areas should be sampled densely and vice versa. To achieve this goal, an adaptive sampling using point laser sensor has been further researched based on isoplanar method for model-unknown surface coordinate metrology. Sampling control points must be previously predicted using the measured data. Therefore, a reference needs to be initially established, and then dynamically updated during sampling process. Isoplanar line method has been employed to plan sampling movement. Curvature-based adaptive step adjustment method and hybrid extrapolation mode have been developed and further employed to calculate the two control increments in both feeding direction and side direction. A group of planar curves, which are utilized as an initial reference for scanning, are primarily sampled in slow tracking stage. As a result, a guide path can be estimated to direct fast scanning for the next path. The surface measurement algorithm was designed and programmed on an open CNC platform. Finally, with the help of linear interpolation technique and macro variables, a practical application has been implemented to verify the proposed fast sampling approach.

Keywords Isoplanar · Adaptive sampling · Sculptured surface · Non-contact · Coordinate metrology

H. Liu (✉) · Y. Wang · X. Huang · L. Xue
Key Laboratory for Precision and Non-traditional Machining Technology of Ministry of Education,
Dalian University of Technology,
Dalian 116024, China
e-mail: haibo_liu@mail.dlut.edu.cn

Abbreviations

CMM	Coordinate measuring machine
CAD	Computer-aided design
CNC	Computer numerical control
NURBS	Non-uniform rational basis spline
3D	Three-dimensional
CEM	Curvature extrapolation mode
TEM	Tangent extrapolation mode
HEM	Hybrid extrapolation mode
MCS	Machine coordinate system
SCS	Sensor coordinate system
PCS	Part coordinate system
BU1	Buffer stack 1
BU2	Buffer stack 2
FSSB	FUNAC serial servo bus
AD	Analog-to-digital converter
NC	Numerical control
PC	Personal computer
VC++	Visual C++
FOCAS1/2	FANUC Open CNC API Specifications version 1 or 2
PMC	Programmable machine controller

1 Introduction

Sculptured surface coordinate methodology that is usually conducted by experienced operators has experimentally proved to be a complex task [1]. The most two important issues are sampling size and the distribution of those points. It is intuitive that the larger the number of points is, the more accurate the reconstruction results are [2]. However, increasing sampling size is associated with longer sampling time, heavier data processing and higher

overall product manufacture cost. A common practice is to distribute sampling points in a uniform pattern. However, a trouble may arise, as unnecessary points are probably measured in flat regions, while some key points in complex regions could be conversely ignored. Taking the surface complexity into consideration, a general principle is that highly curved areas should be measured densely and vice versa. Therefore, optimizing sampling size and point distribution over surface is desirable.

At present, the coordinate pick-up methods can be classified into two categories [3]. One is point-based approach, and the other is scanning approach. In the former process, the sensor needs to stop at a desired control point. Then, it moves rapidly to the next programmed point. By repeating this process, the coordinate information can be obtained point by point. However, since sampling movement is discontinuous, this method is very time consuming. As an alternative approach, scanning technology can continuously acquire coordinate data using contact or non-contact probes. In general, it requires a pre-determined directing path. Isoplanar line method with equal space is always adopted for sculptured surface sampling due to its simplicity of operation. Nevertheless, there is a drawback of being insensitive to different complexity levels [4]. Further, side intervals between adjacent digital planes should be estimated according to local curvature of measured surface.

A great number of literatures on sculptured surface measurement have been reported. Most of these efforts deal with two major subjects: computer-aided design (CAD)-based approach for model-known surface and CAD-independent approach for model-unknown surface. Global and local complexities are employed to plan sampling point distribution in CAD-directed sampling approach. I. Ainsworth employed the CAD model at registration, path planning, and probe radius compensation stages to maximize the measurement accuracy [5]. M. Cho presented an effective planning strategy in on-machine measurement process. At the first step, two point selection methods were discussed considering cutting error or cutter contact points respectively. Then the probe moving distance was minimized by applying the traveling salesman problem algorithm [6]. An iterative sampling process for coordinate measuring machine (CMM) inspection was proposed by R. Edgeworth [7]. Their procedure added new points on the entire profile until all curves that interpolate any two subsequent points were within an acceptable tolerance. D. ElKott studied a hybrid approach to distribute sample points on NURBS parametric surfaces [8]. The surface curvature change and the patch sizes were used to guide sampling process. To find an optimal plan, K.H. Lee researched automatic algorithms for laser scanner-based inspection operations [9]. H.J. Pahk inspected molds with sculptured surface based on three sampling-point strategies, uniform distribution, curvature-dependent distribution, or hybrid distribution [10]. However, defining the sampling size and step length was still an empirical process. K.C. Fan introduced an intelligent inspection path planning of CMM probes for feature-based objects: planar, cylindrical and conical [11]. In contrast, in CAD-independent surface coordinate metrology, the next sampling control point must be previously predicted using the measured points along the measuring direction. At the same time, motion commands will be automatically generated to realize the sampling task. J.C. Lu adopted two control algorithms for tracking mode-unknown surface: constant angular increments algorithm and tangent estimation method [12]. C.K. Song presented an automatic digitization algorithm on a CMM [13]. If the vertex points on polyhedron were precisely measured, the surface model could be easily approximated by triangle plane patches. V. Carbone proposed a novel approach integrating a 3D vision sensor and a CMM to perform reverse engineering of freeform surfaces [14]. Recently, K.Q. Lu presented an adaptive sampling method based on front path detecting [15]. The method was characterized by integration of one-touch probe (capturing coordinate) and two-point laser probes (exploring sampling path). Z.Y. Jia designed a novel data sampling method for freeform surface tracking which combined isochronous indistinctive sampling with off-line equal-error accurate arithmetic [16]. From the researches mentioned above, it is indicated that traditional CAD-based approach has some limitations for model-unknown surface measurement. Consequently, sampling size and point distribution should be reasonably determined according to local geometry of measured surface, whether the reference model has been known or not.

For model-unknown sculptured surface measurement, there are still certain key issues deserving attention. One is sampling control step adjustment. If the local curve segment is approximated by an osculating circle with global minimum curvature radius, more geometric information can be accurately picked up. Nevertheless, a dilemma is that a so small step is employed in gentle surface regions. Similarly, if the sampling step is too large, some key geometric characteristics would be lost. Therefore, the sampling step should be adjusted adaptively according to local curvature. Another is the extrapolating method to predict the next sampling control point. Researches show that there are two extrapolating techniques: curvature extrapolation [17] and tangent extrapolation [18]. The former is very suitable for surfaces with large curvature but with no or little curvature changes, such as circular surface. But if there is a large curvature change, e.g., curvature step, the worst case would come forth. Conversely, if the curvature is very small, such as a plane, the predicting step is so small as to reduce measurement efficiency. For this case, the tangent extrapolation could perform better. Tangent extrapolation method is particularly suitable for flat surface, but when the curvature is large, prediction accuracy of control points will be relatively poor. However, each has its own pros

and cons. In fact, the curvature characteristic of an actual sculptured surface is complex. Hence, a fixed extrapolation method would not be an excellent choice.

Contact or non-contact probes installed in CMM or computer numerical control (CNC) machine are widely employed in various industries [19]. High-precision measurement can be achieved using contact probe. However, low measuring speed, tip wearing, and radius compensation are its main drawbacks. In contrast, non-contact digitizing approach using laser range sensor can meet high efficient measurement requirements.

According to the above discussion, there is a need for an effective method that can adaptively plan sampling size and point distribution for model-known surfaces. Isoplanar line method with unequal space has been employed for sampling points distribution planning. Two sampling increments in both feeding direction and side direction are mainly calculated. A shape function in terms of curvature is constructed to adjust control step from one to q times that user-defined basic arc length. A hybrid extrapolation mode is developed to improve prediction accuracy. As a result, a bridge between constant curvature extrapolation and tangent extrapolation is established according to surface curvature and curvature change rate. Side intervals can be estimated using a conservative criterion. Therefore, a quasi CAD-based sampling process can be realized utilizing the predicted reference points.

To optimize the measuring points on model-unknown sculptured surfaces, an adaptive sampling strategy using non-contact probe has been researched based on isoplanar method in this paper. An isoplanar-based coordinate information extraction principle is described in Section 2. Curvature-based step adaptive adjustment and sampling control point prediction using a hybrid extrapolation mode are mathematically presented respectively in Section 3. Based on the techniques mentioned above, the adaptive sampling algorithm has designed in detail, Section 4. Finally, a practical application was implemented to verify the adaptive sampling approach in Section 5.

2 Isoplanar-based surface sampling principle

Isoplanar-based sampling strategy is a simple and robust sampling approach to extract profile information. Hence, coordinate picking up process will be implemented in Cartesian space. The measured surface is divided into different curves by a set of infinite parallel planes. The parallel planes are called digital planes, and the corresponding plane curves are called digital curves. For each point digitized on a planar curve, the digital planes and curves are fixed relatively to the surface during the digitizing process. The probe is driven from one control point to the following control point using linear interpolation. At the same time, more coordinate information will be extracted by sampling system at a high frequency. The isoplanar-based sampling process is shown in Fig. 1.

Three orthogonal Cartesian systems should be firstly defined. They are machine coordinate system (MCS), sensor coordinate system (SCS) and part coordinate system (PCS). The MCS $\{C_M: X_M, Y_M, Z_M\}$ is defined on machine base. The SCS $\{C_S: X_S, Y_S, Z_S\}$ is defined on reference origin of sensor with Z_S aligning with incident light axis. And the PCS $\{C_P: X_P, Y_P, Z_P\}$ is defined on measured surface. During coordinate metrology, the coordinate points need to be converted from SCS to MSC. In isoplanar-based sampling approach, sensor movement is limited in the digital planes $\{\Pi_j\}$.

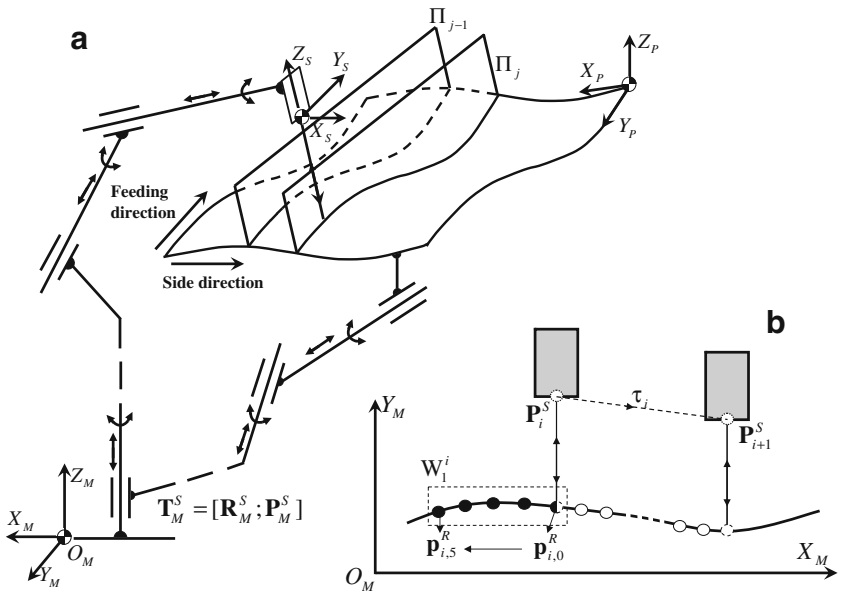

Fig. 1 Isoplanar-based sampling process

The sampling point in SCS is expressed as $\mathbf{p}_S$. The coordinate point can be expressed in MCS using Eq. (1).

$$\left.\begin{aligned}\mathbf{p}_M &= \mathrm{T}_M^S \bullet \mathbf{p}_S \\ \mathbf{p}_S &= (0,0,d_S)^T \\ \mathbf{T}_M^S &= \left[\mathbf{R}_M^S; \mathbf{P}_M^S\right]\end{aligned}\right\} \tag{1}$$

where $\mathbf{p}_M$ denotes coordinate point in MCS. d_S is the displacement range between sensor origin and actual planar curve. $\mathbf{T}_M^S$,$\mathbf{R}_M^S$,$\mathbf{P}_M^S$ denote comprehensive transformation matrix, rotational transformation matrix and translation transformation matrix from SCS to MCS respectively.

In order to illustrate coordinate pick-up process clearly, the digital planes are assumed to be parallel to X_M–Z_M plane, the feeding direction is along X_M-axis and the side direction is along Y_M-direction. The incident light parallels to Z_M-axis. The coordinate point pick-up process is shown in Fig. 1b. In adaptive sampling process, N measured points are used to compute the next control point using an extrapolation method, i.e., a moving reference window W_1. The W_1 width is user-defined. The reference should be updated at a specified time point. Then, the sensor is driven from the ith control point $\mathbf{P}_i^S$ to the $(i+1)$th control point $\mathbf{P}_{i+1}^S$ along linear control path (the dotted line). At the same time, more coordinate points will be automatically picked up at a high frequency. The solid dots and the hollow dots on the measured curve (the solid line) represent the measured points and the points to be collected in the ith sampling step respectively. The dashed dots denote the projection points corresponding to control points. The half-hollow dots mean that it is not sure whether they have been sampled or not. However, it does not matter for the following sampling work.

The i_{th} reference W_1^i is updated by new measured points, from $\mathbf{p}_{i,0}^R$ to $\mathbf{p}_{i,N}^R$. And continuous control points can be determined,

$$\mathbf{P}_{i+1}^S = \mathbf{P}_i^S + \Delta x_i \times \bullet \tau_i \tag{2}$$

where Δx_i is the ith sampling control step. $\tau_i = \overrightarrow{\mathbf{P}_i^S \mathbf{P}_{i+1}^S}$ stands for prediction direction.

Generally, the sensor is driven along a planar curve by a constant sampling speed F. The sampled points denoted by solid dots are picked up by sampling system at the frequency f. Those points can be expressed in MSC,

$$\left.\begin{aligned}\mathbf{p}_{M,k+1} &= \mathbf{p}_{M,k} + \mathbf{T}_k^{k+1} \\ \mathbf{T}_k^{k+1} &= [F\langle \tau_i, k\rangle / f, 0, F\langle \tau_i, i\rangle / f + std_{er}]^T\end{aligned}\right\} \tag{3}$$

where $\mathbf{p}_{M,k}$, $\mathbf{p}_{M,k+1}$ denote the k_{th} and $(k+1)_{\mathrm{th}}$ sampling points respectively. $\mathbf{T}_k^{k+1}$ is a detection translation transformation from the k_{th} point to the $(k+1)_{\mathrm{th}}$ point. std_{er} is a relative displacement error. $\boldsymbol{i}$ and $\boldsymbol{k}$ are the unit vectors of X_M-axis and Z_M-axis respectively.

3 Sampling step adaptive adjustment and control point prediction

For the surface without a reference model, control step determines sampling accuracy and efficiency. Hence, a reasonable step should be chosen.

3.1 Curve geometry using B-spline

To predict the next sampling control point, it is pivotal to construct a local curve segment that can successfully describe actual tendency used a finite number of coordinate points in W_1. B-spline is employed to construct a curve segment for its flexibility and power in representing, and manipulating complex shapes. In fact, cubic B-spline curve is enough to satisfy prediction requirement.

With polynomial equation, a cubic B-spline curve is defined as [20],

$$\left.\begin{aligned}C(u) &= N(u) \bullet Q^T \\ N &= \left[N_{r-N+1,3}(u), \cdots, N_{r-1,3}(u), N_{r,3}(u)\right]_{1\times N} \\ Q &= [Q_{r-N+1}, \cdots, Q_{r-1}, Q_r]_{1\times N}\end{aligned}\right\} \tag{4}$$

where, N is the window width. $\{Q_r\}$ is the collection of control points and $\{N_{r,3}(u)\}$ is the collection cubic B-spline basic functions, derived from DeBoor-Cox recursive formula. u is an independent parameter which is defined in non-uniform knot vector U, $U=\{0,0,0,0,u_4,\ldots,u_{N-1},1,1,1,1\}$.

The first derivation and the second derivation of cubic B-spline are given as follows:

$$\left.\begin{aligned}C'(u) &= N'(u) \bullet Q^T \\ C''(u) &= N''(u) \bullet Q^T\end{aligned}\right\}. \tag{5}$$

Therefore, tangent vector and curvature are then derived using curve differential geometric theory,

$$\mathbf{t}(u) = \frac{(x'(u), z'(u))}{\sqrt{x'(u)^2 + z'(u)^2}} \tag{6}$$

$$\kappa(u) = \frac{|x'(u)z''(u) - x''(u)z'(u)|}{\left[x'(u)^2 + z'(u)^2\right]^{2/3}} \tag{7}$$

Then, tangent angle α relative to X_M-axis can be obtained,

$$\alpha = \cos^{-1}\langle \mathbf{t}, \mathbf{i}\rangle \tag{8}$$

3.2 Curvature-based step adaptive adjustment

The prediction step is adaptively adjusted according to local curvature. Those measured points in W_1^i are interpolated by B-spline. The curvature κ_i of point $\mathbf{P}_i$ is calculated using Eq. (7). Hence, the curvature radius is $R_i=1/\kappa_i$. And tangent angle α_i relative to feeding direction is calculated using Eq. (8). If the sampling step Δx_i is too large, i.e., $\Delta x_i > R_i - R_i \sin\alpha_i$, it leads to sampling distortion, as the beam no longer intersects with actual curve. For a model-unknown surface, a so-called pseudo-global minimum step is given, as follows,

$$\Delta x_{i,\min} = R_{i,\min}\left(\sin\psi - \sin\left|\alpha_{i,\min}\right|\right) \tag{9}$$

where, $R_{i,\min}$ is pseudo-global minimum curvature radius. $\alpha_{i,\min}$ is tangential angle relative to X_M-axis at the corresponding point, and ψ is the maximum allowed surface inclination angle.

The pseudo-global minimum step cannot keep constant. It must be updated with new coordinate points.

A shape function is established to reflect the local surface shape. It can provide quantitative information on which the sampling is based. The function is defined upon curvatures, and its value falls into the range[1,q]. Unlike the linear shape function in Ref. [21], a quadric shape function $\Phi(\kappa_i)$ is derived,

$$\Phi(\kappa_i) = \frac{(q-1)(\kappa_i - \kappa_{\max})^2 + (\kappa_{\max} - \kappa_{\min})^2}{(\kappa_{\max} - \kappa_{\min})^2} \tag{10}$$

where, $q(q>1)$is maximum amplification factor, which is an integer. κ_i is curvature of current sampling point. $\kappa_{\max}$ and $\kappa_{\min}$ are the max and the min curvatures of the measured surface respectively. It should be noted that $\kappa_{\max}$, $\kappa_{\min}$ are continuously updated during sampling process.

As a result, the final sampling step for the current point is,

$$\Delta x_i = \Phi(\kappa_i)\Delta x_{i,\min} \tag{11}$$

Therefore, the basic step is employed in large curvature region, and the sampling step will be enlarged along a quadric curve in gentle region. It means that it adjusts slowly when the curvature is close to the max curvature, otherwise adjusts quickly when the curvature is much smaller than the max curvature.

3.3 Sampling control point prediction

In fact, a fixed extrapolation mode is not an excellent choice for an actual sculptured surface. Thereby, to make best use of the advantages and avoid the disadvantages of both extrapolation approaches is a reasonable decision. There are two prediction error parameters associated with sampling control point prediction, Δd and ΔS. Δd is displacement error between the prediction point and the actual point in Z_S direction. The other arc length error ΔS is related to the prediction arc length and actual arc length. If Δd is too large, the sensor will be out of range and fail to give a displacement reading. And if ΔS is too large, substitute surface reconstruction distortion occurs due to the unreasonable distribution of sampling points. Both of the error parameters are affected by extrapolation mode and prediction step. Therefore, it should carefully take these two errors into account in sampling increment calculation. The scheme diagram of step prediction is shown in Fig. 2.

3.3.1 Curvature extrapolation mode

The basic idea of curvature extrapolation mode (CEM) is that curve segment in the neighborhood of current control point is approximated by a circular arc. Therefore, the next control point can be predicted by curvature circular.

The arc angle θ_i corresponding to basic arc length S at the ith control point is solved using the following equation,

$$\theta_i = S\kappa_i \tag{12}$$

And sampling control step and prediction translation matrix are further derived as follows,

$$\left.\begin{aligned}\Delta x_i &= R_i[\sin\alpha_i + \sin(\theta_i - \alpha_i)]\\ \tau_i &= [1, 0, \tan((\pi - \theta_i)/2 + \alpha_i)]\end{aligned}\right\} \tag{13}$$

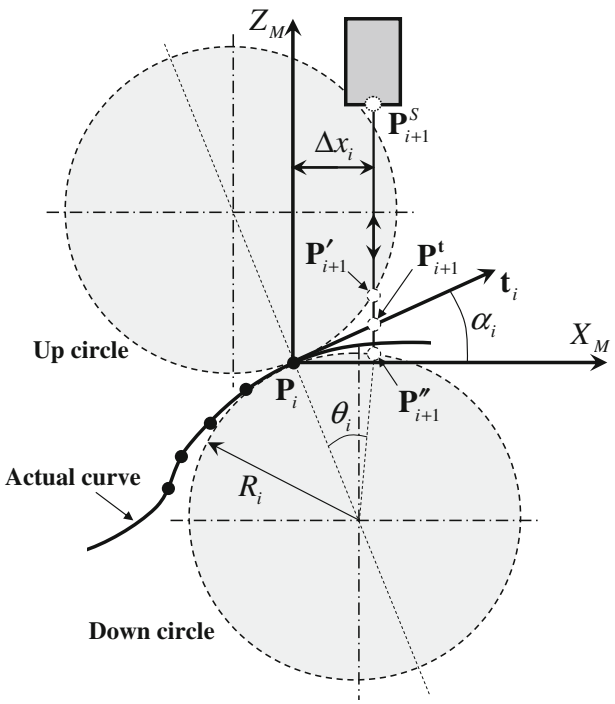

Fig. 2 Scheme diagram of control point prediction

Then, coordinate of the next predicted point in MCS can be obtained using Eq. (2).

Intuitively, the worst case may occur when the extrapolated curve follows the down bounding circle and the digitized curve follows the up bounding circle (or vice versa). Simply, the prediction point is P'_{i+1}, but the actual point is P'_{i+1}. According to plane geometry theory, the mathematical formulations of two error parameter ratios relative to curvature radius are shown,

$$\begin{aligned}\Delta d_i/R_i &= \left|\overrightarrow{P'_{i+1}P''_{i+1}}\right|/R_i \\ &= 2\cos\alpha_i - \sqrt{1-(\sin\alpha_i - \Delta x_i/R_i)^2} \\ &\quad - \sqrt{1-(\sin\alpha_i + \Delta x_i/R_i)^2}\end{aligned} \tag{14 - a}$$

$$\begin{aligned}\Delta S_i/R_i &= \left(\widehat{P_iP''_{i+1}} - \widehat{P_iP'_{i+1}}\right)/R_i \\ &= \pi/2 - 2|a_i| + \sin^{-1}(\sin(|a_i|) - \Delta x_i/R_i) \\ &\quad - \cos^{-1}(\sin(|a_i|) + \Delta x_i/R_i)\end{aligned} \tag{14 - b}$$

3.3.2 Tangent extrapolation mode

As shown in Fig. 2, if tangent extrapolation mode (TEM) is employed, the prediction point is $\mathbf{P}^{\mathbf{t}}_{i+1}$. The basic tangential step is T. Sampling control step and prediction translation matrix are described as,

$$\left.\begin{aligned}\Delta x_i &= T\cos\alpha_i \\ \tau_i &= [1, 0, \tan\alpha_i]\end{aligned}\right\} \tag{15}$$

In fact, the next sampling point may not be on the tangential line, for instance locating at up circular or down circular. However, in the worst case, the prediction errors are decreased compared to that in CEM, because the extrapolation point is placed in the middle of the locally bounded region. Therefore, the possible displacement error ratio and the arc length error ratio are formulated as,

$$\begin{aligned}\frac{\Delta d'_i}{R_i} &= \frac{\left|\overrightarrow{P^t_{i+1}P'_{i+1}}\right|}{R_i} \\ &= \cos\alpha_i - \sqrt{1-(\sin\alpha_i - \Delta x_i/R_i)^2} + \sin\alpha_i \Delta x_i/R_i\end{aligned} \tag{16 - a}$$

$$\begin{aligned}\frac{\Delta d''_i}{R_i} &= \frac{\left|\overrightarrow{P^t_{i+1}P''_{i+1}}\right|}{R_i} \\ &= \cos\alpha_i - \sqrt{1-(\sin\alpha_i + \Delta x_i/R_i)^2} - \sin\alpha_i \Delta x_i/R_i\end{aligned} \tag{16 - b}$$

$$\begin{aligned}\frac{\Delta S'_i}{R_i} &= \frac{\widehat{P_iP'_{i+1}} - \widehat{P_iP^t_{i+1}}}{R_i} \\ &= |a_i| - \sin^{-1}(\sin(|a_i|) - \Delta x_i/R_i) \\ &\quad - \Delta x_i/R_i\cos a_i\end{aligned} \tag{16 - c}$$

$$\begin{aligned}\frac{\Delta S''_i}{R_i} &= \frac{\widehat{P_iP''_{i+1}} - \widehat{P_iP^t_{i+1}}}{R_i} \\ &= \pi/2 - \sin|a_i| - \cos^{-1}(\sin(|a_i|) \\ &\quad + \Delta x_i/R_i) - \Delta x_i/R_i\cos a_i\end{aligned} \tag{16 - d}$$

3.3.3 Hybrid extrapolation mode

It is obvious that two extrapolation modes have their limitations. In another words, both two methods are complementary. This motivates the development of a reasonable extrapolation mode, the so-called hybrid extrapolation mode (HEM). The local geometry is characterized by curvature and curvature change rate. The former can be calculated using Eq. (7), and the curvature change rate is derived as follows,

$$\begin{aligned}\varsigma_i(u) = \frac{d\kappa_i(u)}{du} &= \frac{x'_i(u)z'''_i(u) - x'''_i(u)z'_i(u)}{\left[x'_i(u)^2 + z'_i(u)^2\right]^{2/3}} - 3\kappa_i(u) \\ &\quad \times \frac{x'_i(u)z''_i(u) + x''_i(u)z'_i(u)}{x'_i(u)^2 + z'_i(u)^2}\end{aligned} \tag{17}$$

According to the above analysis, CEM can satisfy prediction requirement of the segments with large curvature and little curvature change. In contrast, TEM is a better choice for plane segments. Two threshold values are defined, curvature error δ_κ and curvature change error δ_ς. The pseudo-code of HEM is,

(1) IF $\kappa_i < \delta_\kappa$ or $\varsigma_i > \delta_\varsigma$, Choose TEM;
(2) ELSE, Choose CEM.

4 Surface adaptive sampling algorithm

4.1 Architecture of adaptive sampling algorithm

The architecture of the proposed adaptive sampling is shown in Fig. 3, which mainly includes three functional modules: initialization module, slow tracking module and fast scanning module. Logical relationship between those functional modules is described by thin solid arrow lines.

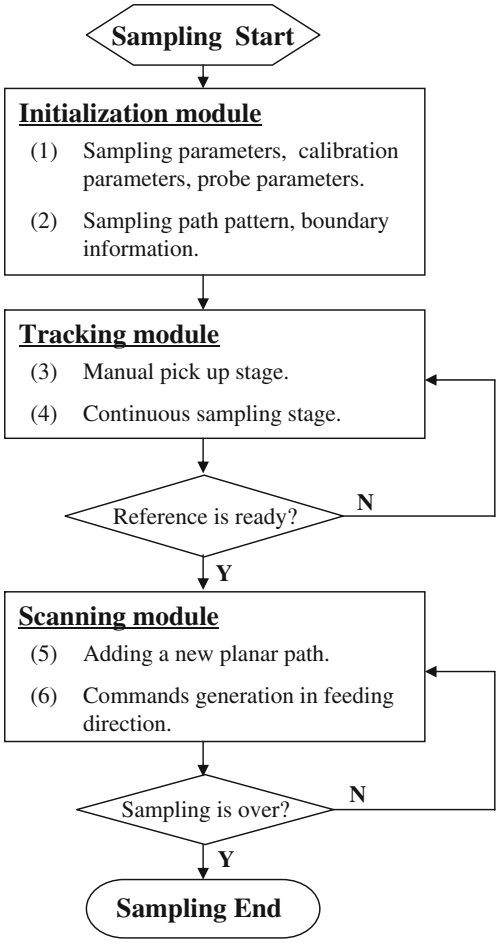

Fig. 3 Flowchart of adaptive sampling algorithm

In the initialization module, the sampling parameters, calibration parameters and sensor parameters are initialized in sampling system. The sampling parameters include tracking speed, scanning speed, and control distance between sensor and measured surface, etc. In order to ensure the accuracy consistency of capturing sampling data, a reasonable stable range should be set. Lower and upper bounds are pre-defined according to sensor working range and standoff distance. In order to register the coordinate point in MCS, a sensor calibration process must be conducted to obtain the deviation relative to the origin of MCS. Generally, zig-zag path strategy is willingly adopted. In this research, it is assumed that the measured surface is a ruled quadrilateral region surface. Hence, the boundaries should be detected before sampling. Then the boundary coordinate information is used to direct the start and the end of sampling movement.

The second module, tracking module, is mainly used to obtain an initial reference for fast scanning. A group of planar curves will be measured. Hence, a pattern with small equal side interval can be formed. A slowing tracking method is used to acquire each planar curve. A reference generated from previous measurements should be dynamically updated. The initial N reference points need to be picked up by manual operation. It is named manual pick-up stage. Since the dynamic reference has been established using a moving window W_1 of N immediate previous points, the planar curves can be continuously sampled at a tracking speed.

Scanning module is the kernel of surface adaptive sampling, which is mainly composed of side increment calculation, scanning path generation and dynamic reference update. M planar curves have been obtained in tracking module. Therefore, side increments can be estimated using curvature-based step adaptive adjustment method and HEM. As a result, a group of reference points are obtained in Cartesian space. The next reference scanning path will be formed after further interpolation using B-spline technology. In fact, there are some deviations between actual curve and reference path. If a reasonable side interval reflecting local curvature characteristics has been provided, the bad effect of deviations could be ignored. Then, the reference should be updated by adding a new planar curve. Therefore, a quasi CAD-based fast scanning has been realized.

4.2 Track sampling

In this process, M planar curves will be measured as an initial scanning reference. For each planar curve, N previous reference points are picked up by manual operation in the manual pick-up stage. And the sensor can then be driven by the next predicted control point at a tracking speed. The reference will be dynamically updated when the sampling system emits a signal at a specified time point.

4.2.1 Manual pick-up

The sensor is driven to each reference point in jog or handle mode. Before detecting a point, it should be moved to a safe position and adjusted in incident beam direction, such that the surface lies in the stable working range. Then, the initial point coordinates are picked up through a conversion from SCS to MCS. A manual step is determined by trial and error. It is assumed that the surface variations are not large enough to result in a measurement failure.

4.2.2 Continuous tracking

To ensure continuous tracking motion, the synchronization between data collection rate and computational time for the dynamic reference is required. In this stage, two main tasks must be completed within the specified time: (1) generating feeding step to guide tracking movement, (2) determining a signal point to load reference update and step prediction procedures.

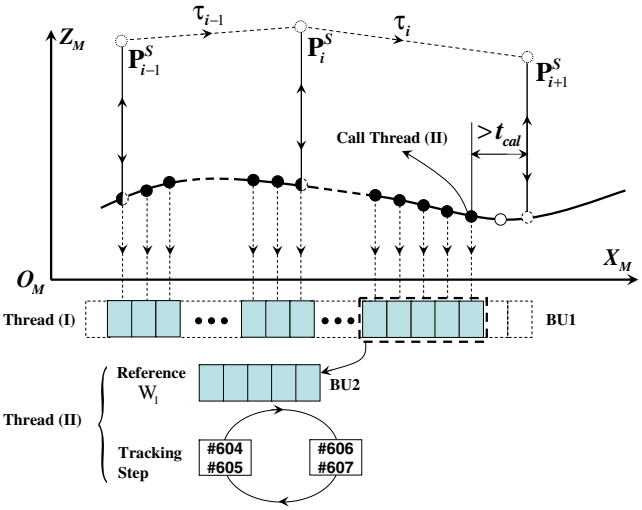

Fig.4 Track sampling process

The continuous tracking process based on a moving window W_2 is shown in Fig. 4. The control direction may be along a tangential extrapolation direction or a curvature extrapolation direction according to HEM. The control points and the displacement deviations are acquired at the same time. The sampled points are continuously stored in a buffer stack 1 (BU1) with a defined length. For example, it can satisfy the number requirement of two adjacent steps at least. When the signal is awakened, the older reference in buffer stack 2 will be dynamically updated using the latest reference points. Then, the next control point is predicted. Four macro variables have been employed to store the current step and the next step respectively, #604 and #605, #606 and #607. They are formed a circle list when the two steps are called circularly in sampling program.

The next problem is to determine the signal point. It should satisfy the following condition,

$$\frac{\left(x_i^C + \Delta x_i - x_i\right)\sqrt{\Delta x_i^2 + \Delta z_i^2}}{\Delta x_i F_T} > t_{\text{cal}} \tag{18}$$

where x_i^C is coordinate of the ith control point. x_i is signal coordinate. Δx_i and Δz_i denote the current control steps in X_M- and Z_M- directions respectively. F_T is tracking speed. t_{cal} denotes the total calculation time of reference update, step calculation and writing time. In practice, the magnitude of t_{cal} depends on the computing power and communication speed. This is natural that the smaller the calculation time is, the faster the tracking speed will be.

4.3 Fast scanning

The moving window W_2 of M previous planar curves is employed as a reference to estimate side intervals. The

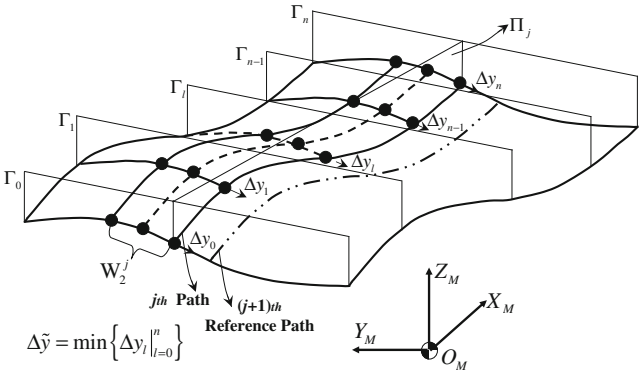

Fig. 5 Fast scanning process

measured planar curves in W_2 are partitioned by a group of digital planes which are orthogonal to feeding direction, $\{\Gamma_l\} l = 0, 1, \ldots, n$.

Similar to tracking control point prediction, the side interval in each orthogonal planar curve can be predicted. Hence, a reference scanning path is formed for the next

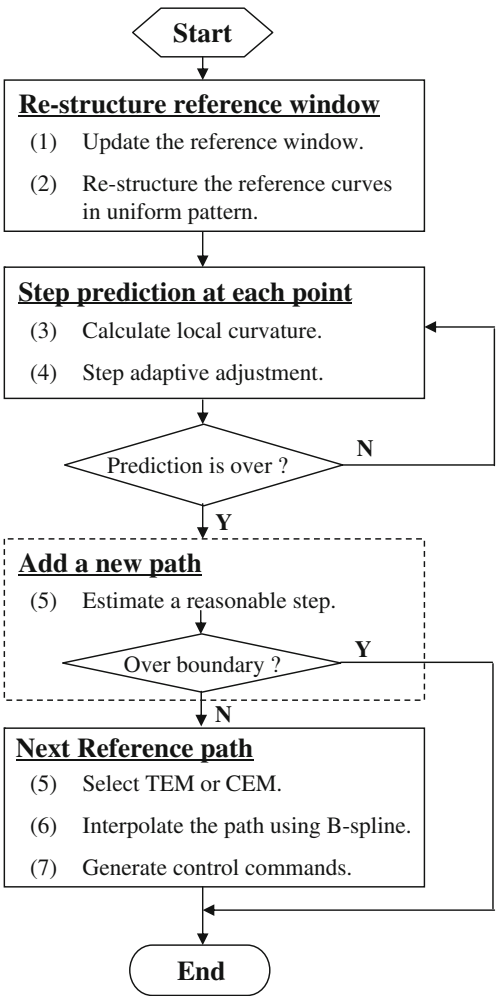

Fig. 6 Flow chart of side interval calculation

planar curve using the predicted points. However, the reference path should be further processed using numerical technology to produce sampling control points. From this point of view, a quasi CAD-based fast scanning has been realized. After a planar curve is measured, the reference W_2 should be updated dynamically. The fast scanning schematic diagram is shown in Fig. 5. The measured curves are described using thick solid lines. The omitted curves in middle area are depicted by dotted lines. And, the predicted reference path is expressed by double-dotted lines.

4.3.1 Side intervals

Sampling points are not uniformly distributed on each planar curve in W_2. Thereby, the digital curves cannot be directly used to predict side interval. They should be restructured in a regular form. The flow chart for side interval calculation is shown in Fig. 6.

The side interval calculation is conducted between the current curve and the following curve. In the l_{th} orthogonal digital plane, the side interval is estimated using curvature-based step adaptive adjustment approach and HEM, which have been described in section 4. Like this, one plane by one plane, a group of candidate value can be obtained, $\{\Delta y_l\}$. To avoid missing certain important points on measured surface, the side path interval is conservatively selected,

$$\begin{cases} y_{j+1} = y_j + \Delta\widetilde{y} \\ \Delta\widetilde{y} = \min\left\{\Delta y_l|_{l=0}^{n}\right\} \end{cases} \tag{19}$$

where, y_j and y_{j+1} are the jth and the $(j+1)$th curve path coordinate values. Δ is the estimated path interval.

In order to calculate the reference point, the estimated path step Δ should be re-taken into the extrapolation mode. Therefore, the $(j+1)_{\text{th}}$ sampling reference path can be obtained.

4.3.2 Control points in feeding direction using equal chord error

The reference sampling path is approximated by small segments using B-spline interpolation technology. The redundant data points should be removed by checking the approximation error to ensure that the selected sampling control points can meet equal chord error requirement. The algorithm structure is described as follows: (1) calculate a maximum chord height of all middle points between the selected current control point and the next quasi-control point; (2) if the max chord height is smaller than the set accuracy value, move to the next quasi-control point; (3) if the max chord height is not smaller than the set accuracy value, record the former point of the quasi-control point; (4) repeat the cycle until the end of the selection process.

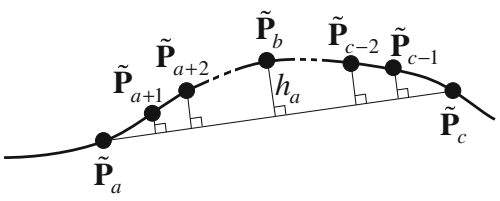

Fig. 7 Chord error

The equal error control points calculation is shown in Fig. 7. The chord height is formulated as,

$$h_b = \left| \left(\widetilde{\mathbf{P}}_b - \widetilde{\mathbf{P}}_a\right) - \frac{\left(\widetilde{\mathbf{P}}_b - \widetilde{\mathbf{P}}_a\right) \bullet \left(\widetilde{\mathbf{P}}_c - \widetilde{\mathbf{P}}_a\right)}{\left(\widetilde{\mathbf{P}}_c - \widetilde{\mathbf{P}}_a\right)^2} \left(\widetilde{\mathbf{P}}_c - \widetilde{\mathbf{P}}_a\right) \right| \tag{20}$$

where, h_b is chord height of middle points $\widetilde{\mathbf{P}}_b (b = a+1, \cdots, c-1)$. $\widetilde{\mathbf{P}}_a$, $\widetilde{\mathbf{P}}_c$ denote the current control point and the quasi-control point respectively, $c > a \geq 0$.

4.4 Adaptive sampling algorithm

Before the adaptive sampling implementation, those important parameters should be determined in parameter module, such as tracking speed, scanning speed, manual step, basic tracking step signal time point, basic side step, and so on. In the adaptive sampling algorithm, tracking and scanning are mainly conducted. Two threads have been programmed: the thread (I) keeps working in the whole sampling process to pick up coordinate points; the thread (II) is only awakened at some specified time points. The adaptive sampling process is divided into some steps as follows:

Step 1. Unidirectional zig-zag pattern is adopted. Four boundaries are firstly detected. The first planar curve is selected. Jump to Step 2.

Step 2. The selected curve will be sampled at a tracking speed. Initial N points are picked up by manual operation, $\left[P_{i,0}\right]_{i=0}^{N-1}$. Then, those points are interpolated by B-spline. The curvatures at each point will be calculated, $\kappa_{\max}$ and $\kappa_{\min}$ are estimated. The first tracking control point can be predicted. Start the track sampling procedure. Meanwhile, thread (I) is awakened and the sampling points are stored in BU1. Then, thread (II) is awakened at the specified time point. Therefore, the dynamic reference will be updated; the following tracking control point is calculated. One point by one point, the profile information of the whole planar curve

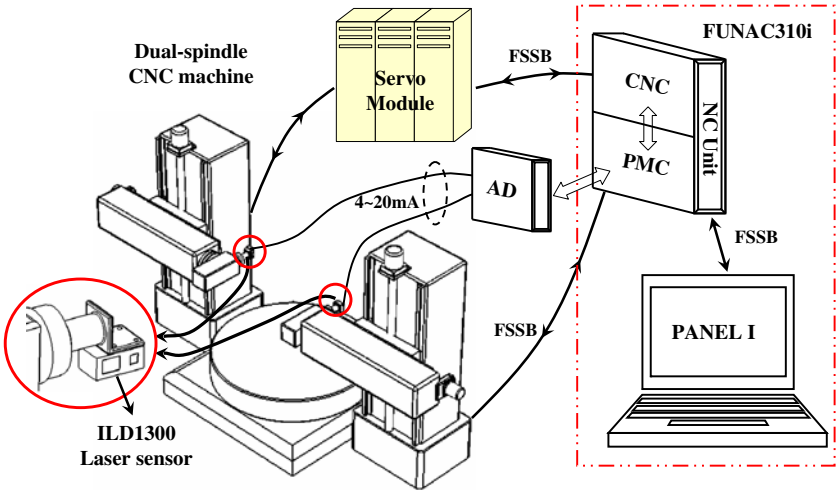

Fig. 8 Hardware architecture of sampling system

can be obtained. If one planar curve sampling has been completed, jump to Step 3.

Step 3. If the number of tracking planar curves can meet the requirements for fast scanning, jump to step 4. Otherwise, return to step 2.

Step 4. The planar curves in W_2 are re-structured in uniform pattern. Like in tracking process, each orthogonal planar curve is interpolated by B-spline. The curvatures at each point are calculated, $\kappa_{\max}$ and $\kappa_{\min}$ are updated. Then one side interval can be estimated in current orthogonal plane. A group of side intervals are then obtained through the above process. Then, a minimum side interval is estimated. Therefore, the reference points can be calculated using the estimated side interval. Jump to step 5.

Step 5. A reference sampling path can be formed by interpolating those predicted points using B-spline for the next planar curve. A set of scanning control points are then determined according to equal chord error constrain. The scanning G codes are generated and transmitted to sampling system. With sensor being driven along the reference scanning path, the following planar curve will be

Fig. 9 NC codes of surface adaptive sampling

```
O1000 –Main Program
N10 G90 G00 Y#501 Z#502 B#503;
N20 M98 P#5071001;
N30 M102;
N40 G00 Y#501 Z#502 B#503;
N50 M98 P1002;
N60 M02;
```

```
O1002 –Scanning
N10 M103;
N20 IF [#703 LT #509]  GOTO 130;
N30 IF [#611 EQ #610] GOTO 100;
N40 G01 Y#701 Z#702 B#703
      F#520;
N50 #611=#611+1;
N60 #701=#[701+#611*3];
N70 #702=#[702+#611*3];
N80 #703=#[703+#611*3];
N90 GOTO 30;
N100 G00 Z#502;
N110 Y#501;
N120 GOTO 10;
N130 M99;
```

```
O1001 –Tacking
N10 M101;
N20 G00 Y#504 Z#505 B#506;
N30 WHILE [#602 LT #511] DO 1;
N40 IF [#600 EQ 1] GOTO 100;
N50 #601= #601+#604;
N60 #602= #602+#605;
N70 G01 Y#601 Z#602 F#500;
N80 #600=1;
N90 GOTO 30;
N100 #601= #601+#606;
N110 #602= #602+#607;
N120 G01 Y#601 Z#602;
N130 #600=0;
N140 GOTO 30;
N150 END 1;
N160 M99;
```

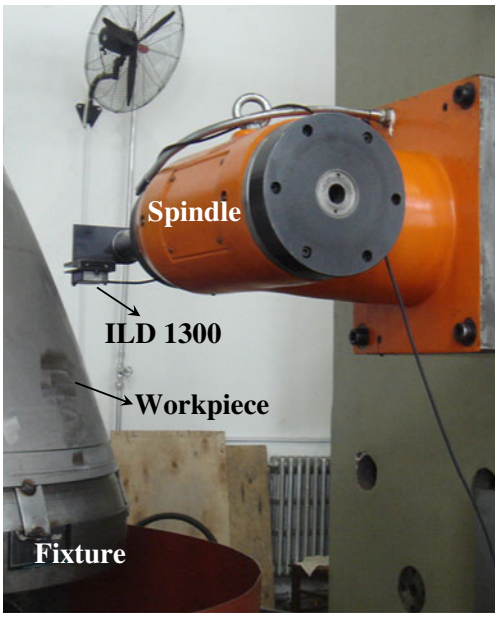

Fig. 10 A practical application

sampled. If the current planar curve has been completed, jump to step 6.

Step 6. If the whole surface measurement is not completed, update the dynamic reference W_2. Jump to Step 4. Otherwise, end the sampling procedure.

5 Experiments

A practical experiment has been designed to (a) determine the effect of user variables on the sampling result and (b) validate the method for slow tracking and fast scanning on a real setup.

The experimental apparatus used in this study includes a dual-spindle CNC machine, two MICRO-EPSILON ILD1300 laser displacement sensors, FANUC 310i control system, shown in Fig. 8.

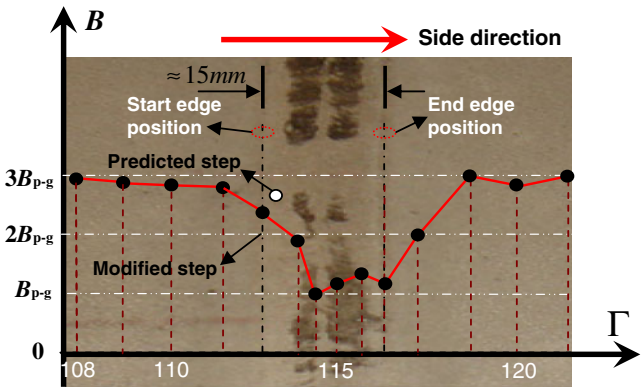

Fig. 11 Side interval steps in the welding region

The special CNC machine has been designed for surface adaptive metrology. The laser sensors are mounted on the two spindles with special fixtures. Because the five servo axes are controlled using dual-channel mode, unilateral sampling using only a single spindle and symmetry sampling using two spindles are available. The FANUC 310i CNC system is composed of PANEL I (i.e., upper PC) and NC unit. The CNC system was used to control sampling movement through FSSB and to collect sensor data through analog-to-digital converter board (i.e., AD board).

The laser sensor has a standoff distance of 100 mm, a measurement range of ±50 mm, a spot diameter at middle range of 0.13 mm, a static resolution of 0.025 mm, the measuring rate of 500 HZ, and a linearity of ±0.2 % of a measurement range of 100 mm.

The surface adaptive sampling system has been built using VC++6.0 supplied by Microsoft Corporation. An open function library, FOCAS1/2, was utilized to establish the communication between PANEL I and NC unit. Some important parameters can be read or written by upper PC in real time, such as PMC parameters, CNC parameters, macro variables and so on. Therefore, surface slow track sampling and fast scanning can be realized on a CNC machine. The basic NC procedures of tracking and scanning are programmed using linear interpolation technology and macro variables, shown in Fig. 9.

Tracking speed, scanning speed and reference width of W_2 were stored in #500, #520, and #507. Four boundaries of the measured surface were recorded in #508, #509, #510, and #511, respectively. Three-dimensional coordinates of global reference point and tracking reference point were pre-determined in two ranges, from #501 to #503 and from #504 to #506. A tracking control flag in # 600 has been designed guiding to the next tracking control point. The coordinates of tracking control point from #601 to #603 should be dynamically updated in tracking process. Step components in feeding direction and laser incident direction of the current interpolation segment and the next interpolation segment were dynamically updated in #604 and #605,

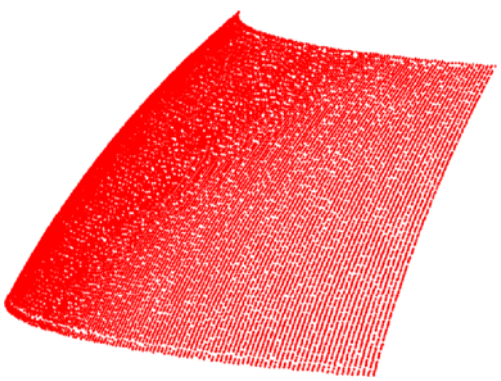

Fig. 12 Plot part of raw sampling points

and in #606 and #607, respectively. The total number of scanning control points for each planar curve was stored in #610. And the corresponding index number was #611. A very wide data memory from #701 to #999 was used to store scanning control points of each scanning planar curve. Finally, three ready signals have been defined, M101 for tracking, M102 for scanning, and M103 for the next scanning path.

To illustrate a practical application of this digitizing system, a large complex workpiece was digitized using the proposed adaptive sampling approach, shown in Fig. 10. Some important sampling parameters are, tracking speed 500 mm/min, scanning speed 4,000 mm/min, sampling frequency 125 HZ, axis displacement deviation of signal point relative to each end point 1 mm in tracking process, basic control step 5 mm, control distance between sensor and surface 60 mm, sensor stable range ±1 mm.

The raw sampling surface data were collected in cylindrical coordinate system since the experimental workpiece was an approximate revolution surface. In another way, the control step was rotation angle B_j instead of a linear coordinate increment Δy_j. Hence, an additional transformation should be constructed during sampling control step prediction. There were several welded seams on the experimental workpiece. The width of welding region was about 15 mm. The angle steps in side direction have been adaptively adjusted, shown in Fig. 11. The horizontal axis and the vertical axis are the number of digital planes and angle steps B respectively. In this region, the CEM has been mainly adopted, because both the curvature κ and the curvature change rate ς were larger than the corresponding threshold values. The width of moving window W_2M was 5. The maximum multiple q was 3. The minimum pseudo-global angle step $\boldsymbol{B}_{\text{p-g}}$ was 0.0105 rad. In Fig. 11, it can be seen that the angle step was close to the maximum $3\boldsymbol{B}_{\text{p-g}}$ before entering or after leaving the welding region because the local curvature was close to constant. And the angle steps changed from $3\boldsymbol{B}_{\text{p-g}}$ to basic step $\boldsymbol{B}_{\text{p-g}}$ according to curvature changing in welding region. However, the minimum angle step has not always been kept since part of welding region has been manually refaced before measuring. Further, the measured points had certain influence on the first control step prediction after leaving the welding region.

Welding region was a stepped structure of the measured surface. The stepped edges could not been directly found using the proposed sampling algorithm in Part 4. In other words, the stepped edge position should be manually determined, such as the angle position of the welding region. Further, the pre-determined edge position was used to decide control step around stepped regions. If the predicted step (the hollow point in Fig. 11) were too large to cross the edge, the edge position was employed to calculate a new control step, or called modified control step, shown in Fig. 11.

In the subsequent data processing, the measured coordinate points should be transformed from cylindrical coordinate system to Cartesian coordinate system for surface construction. Parts of the digitized data were potted in Fig. 12, containing 20,140 points.

6 Conclusions

In this article, an adaptive sampling of model-unknown sculptured surface has been developed based on isoplanar line method.

1. Two key issues have been effectively solved. A quadric shape function in terms of curve curvature was constructed to adaptively adjust control step. Another, a hybrid extrapolation mode (HEM) was researched according to surface complexity.
2. In order to predict the control points in feeding direction and side direction respectively, W_1 and W_2 were established as the reference windows. Therefore, the point laser sensor was driven by control points using linear interpolation technology. At the same time, more actual coordinate points were automatically picked up by sampling system at a high frequency.
3. A surface adaptive sampling system has been built on FANUC310i system using Visual C++6.0 supplied by Microsoft Co. and FOCAS1/2 supplied by FANUC Co. In PANEL I, PMC parameters, CNC parameters and macro variables, could be read or written by in real time. Therefore, surface slow track sampling and fast scanning could be realized on a CNC machine.
4. A large complex workpiece with certain welded seams has been digitized to verify the validation of the proposed approach on a special machine. Two MICRO-EPSILON ILD1300 laser displacement sensors were employed in the experiment. The surface fast sampling NC procedures were conducted using G codes and macro variables. The scanning speed achieved 4,000 mm/min. In order to precisely measure a stepped structure, such as a welding region, the pre-determined edge position was employed to modify the predicted angle step.

Acknowledgement This project is supported by National Natural Science Foundation of China (Key Program grant no. 50835001) and Advanced research Foundation (Key Program grant no. 9140A18020310JW0902).

References

1. Vezzetti E (2009) Adaptive sampling plan design methodology for reverse engineering acquisition. Int J Adv Manuf Technol 42(7–8):780–792. doi:10.1007/s00170-008-1625-z
2. Hocken RJ, Raja J, Babu U (1993) Sampling issues in coordinate metrology. ASME Manuf Rev 6(4):282–294
3. Li DY, Gu PH (2004) Free-form surface inspection techniques state of the art review. Comput Aided Des 36:1395–1417. doi:10.1016/j.cad.2004.02.009
4. ElKott D, Veldhuis S (2005) Isoparametric line sampling for the inspection planning of sculptured surfaces. Comput Aided Des 37:189–200. doi:10.1016/j.cad.2004.06.006
5. Ainsworth I, Ristic M, Brujic D (2000) CAD-based measurement path planning for free-from shapes using contact probes. Int J Adv Manuf Technol 16(1):23–31. doi:10.1007/PL00013128
6. Cho M-W, Seo T-I (2002) Inspection planning strategy for the on-machine measurement process based on CAD/CAM/CAI integration. Int J Adv Manuf Technol 19(8):607–667. doi:10.1007/s001700200066
7. Edgeworth R, Wilhelm R (1999) Adaptive sampling for coordinate metrology. Precis Eng 23:144–154. doi:10.1016/S0141-6359(99)00004-5
8. ElKott D, ElMaraghy H, ElMaraghy W (2002) Automatic sampling for CMM inspection planning of free form surfaces. Int J Prod Res 40:2653–2676. doi:10.1080/00207540210133435
9. Lee KH, Park HP (2000) Automated inspection planning of free-form shape parts by laser scanning. Robot Comput Integr Manuf 16(4):201–210. doi:10.1016/S0736-5845(99)00060-5
10. Pahk HJ, Jung MY, Hwang SW, Kim YH, Hong YS, Kim SG (1995) Integrated precision inspection system for manufacturing of moulds having CAD defined features. Int J Adv Manuf Technol 10(3):198–207. doi:10.1007/BF01179348
11. Fan KC, Leu MC (1998) Intelligent planning of CAD-directed inspection for coordinate measuring machines. Comput Integr Manuf Syst 11(1–2):43–51. doi:10.1016/S0951-5240(98)00008-1
12. Lu JC, Duffle NA, Bollinger JG (1982) Two dimensional tracing and measurement using touch trigger probes. CIRP Ann 31(1):415–419. doi:10.1016/S0007-8506(07)63339-3
13. Song CK, Kim SW (1997) Reverse engineering: autonomous digitization of free formed surfaces on a CNC coordinate measuring machine. Int J Mach Tools Manuf 37(7):1041–1051. doi:10.1016/S0890-6955(96)00059-4
14. Carbone V, Carocci M, Savio E, Sansoni G, Chiffre LD (2001) Combination of a vision system and a coordinate measuring machine for the reverse engineering of freeform surfaces. Int J Adv Manuf Technol 17(4):263–271. doi:10.1007/s001700170179
15. Lu KQ, Wang W, Chen ZC (2010) Adaptive sampling of digitizing for the unknown free-form surface based on front path detecting. Chin J Mech Eng 46(9):143–149
16. Jia ZY, Lu XH, Wang W, Yang JY (2010) Data sampling and processing for contact free-form surface scan-tracking measurement. Int J Adv Manuf Technol 46(1–4):237–251. doi:10.1007/s00170-009-2083-y
17. Smith KB, Zheng YF (1994) Multi-laser displacement sensor used in accurate digitizing technique. ASME J Eng Ind 116:482–490. doi:10.1115/1.2902132
18. Hu J, Li Y, Wang YH, Cai JG (2004) Adaptive sampling method for laser measuring free-form surface. Int J Adv Manuf Technol 24(11–12):886–890. doi:10.1007/s00170-003-1802-z
19. Zhang GX (1999) Coordinate measuring machines. Tianjin University Press, Tianjin
20. Li SZ (1995) Adaptive sampling and mesh generation. Comput Aided Des 27:235–240. doi:10.1016/0010-4485(95)95872-C
21. Piegl L, Tiller W (1997) The NURBS Book, 2nd edn. Springer, Berlin